2011

Electronic interactions within composites of polyanilines formed under acidic and alkaline conditions. Conductivity, ESR, Raman, UV-vis and fluorescence studies

L Dennany
University of Wollongong, lynnd@uow.edu.au

P C. Innis
University of Wollongong, peter_innis@uow.edu.au

S T. McGovern
University of Wollongong, scottmcg@uow.edu.au

Gordon G. Wallace
University of Wollongong, gwallace@uow.edu.au

Robert J. Forster
Dublin City University, robert.forster@dcu.ie

Electronic interactions within composites of polyanilines formed under acidic and alkaline conditions. Conductivity, ESR, Raman, UV-vis and fluorescence studies

Abstract

The properties of two forms of polyaniline (PAni) synthesised under acidic and basic conditions have been investigated both individually and as combined complexes. The PAni polymerised within alkaline media was redox inactive and non-conducting while the PAni emeraldine salt (ES) was electroactive and conducting. Raman, electron spin resonance, UV-Vis and fluorescence spectroscopies were used to monitor the changes in electronic properties of these conducting polymer composites. Solution cast films of alkaline synthesised (A-PAni) with the PAni ES resulted in an increase in the high spin polaron population suggesting that it acts as a pseudodopant. The ability of the A-PAni to increase and maintain the population of the polaron charge carrier was confirmed by UV-vis and Raman spectroscopy. Significantly, the presence of the A-PAni in PAni ES helped to sustain higher electrical conductivities at loading levels that were well below the percolation threshold of an insulating polystyrene sulfonate polymeric oligomer model. Fluorescence studies indicated that the A-PAni was fluorescent. However, mixtures of A-PAni with the PAni ES resulted in quenching of the A-PAni emission. The quenching process was observed to involve both static and dynamic processes, with the static quenching being dominant. These results suggest that the two polymers are strongly associated with each other when in the solid state. In stark contrast, the alkaline synthesized PAni did not influence the electrochemical properties of the emeraldine salt. These results deviate significantly from the expected outcome of the addition of an insulating A-PAni additive and highlight the unusual interactions occurring between PAni and its alkaline analogue. © the Owner Societies 2011.

Keywords

within, interactions, electronic, formed, alkaline, acidic, conditions, conductivity, polyanilines, esr, raman, uv, vis, fluorescence, studies, under, composites

Disciplines

Life Sciences | Physical Sciences and Mathematics | Social and Behavioral Sciences

Publication Details

Dennany, L., Innis, P. C., McGovern, S. T., Wallace, G. G. & Forster, R. J. (2011). Electronic interactions within composites of polyanilines formed under acidic and alkaline conditions. Conductivity, ESR, Raman, UV-vis and fluorescence studies. Physical Chemistry Chemical Physics, 13 (8), 3303-3310.

PCCP

Cite this: *Phys. Chem. Chem. Phys.*, 2011, **13**, 3303–3310

www.rsc.org/pccp

PAPER

Electronic interactions within composites of polyanilines formed under acidic and alkaline conditions. Conductivity, ESR, Raman, UV-vis and fluorescence studies†

L. Dennany,[a] P. C. Innis,*[a] S. T. McGovern,[a] G. G. Wallace[a] and Robert J. Forster[b]

Received 27th May 2010, Accepted 23rd November 2010
DOI: 10.1039/c0cp00699h

The properties of two forms of polyaniline (PAni) synthesised under acidic and basic conditions have been investigated both individually and as combined complexes. The PAni polymerised within alkaline media was redox inactive and non-conducting while the PAni emeraldine salt (ES) was electroactive and conducting. Raman, electron spin resonance, UV-Vis and fluorescence spectroscopies were used to monitor the changes in electronic properties of these conducting polymer composites. Solution cast films of alkaline synthesised (A-PAni) with the PAni ES resulted in an increase in the high spin polaron population suggesting that it acts as a pseudodopant. The ability of the A-PAni to increase and maintain the population of the polaron charge carrier was confirmed by UV-vis and Raman spectroscopy. Significantly, the presence of the A-PAni in PAni ES helped to sustain higher electrical conductivities at loading levels that were well below the percolation threshold of an insulating polystyrene sulfonate polymeric oligomer model. Fluorescence studies indicated that the A-PAni was fluorescent. However, mixtures of A-PAni with the PAni ES resulted in quenching of the A-PAni emission. The quenching process was observed to involve both static and dynamic processes, with the static quenching being dominant. These results suggest that the two polymers are strongly associated with each other when in the solid state. In stark contrast, the alkaline synthesized PAni did not influence the electrochemical properties of the emeraldine salt. These results deviate significantly from the expected outcome of the addition of an insulating A-PAni additive and highlight the unusual interactions occurring between PAni and its alkaline analogue.

Introduction

Polyaniline (PAni) prepared in acidic media is one of the most widely studied conducting polymers due to its straightforward method of preparation and the stability of its conductive emeraldine salt (ES) form (Scheme 1).[1,2] Many applications have been examined, including their use in energy storage media, electrochromic devices, chemical sensors and as actuators.[3–6]

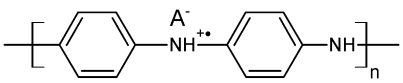

Scheme 1 Structure of PAni emeraldine salt.

More recently studies have been directed towards the synthesis of these materials at the nanoscale with one notable route reported by the Stejskal research group.[7] These studies have reported the formation of nanostructures from the oxidation of aniline monomer under alkaline conditions.[8–11] These structures have been identified to be phenazine-like oligomers unlike those formed *via* synthesis of PAni in acidic media. These novel oxidation products from the alkaline oxidative polymerisation of aniline (A-PAni) may gain considerable significance due to their exceptional electronic properties and also their contributions to the field of nano/micro science such as hollow nanospheres.[12,13] These future potential applications still require in-depth understanding of the unique properties and interactions of these materials. This is particularly important given the many subtle synthetic variations that occur during the synthesis of PAni with the potential to form mixtures of the emeraldine salt and phenazine base oligomers of PAni.

[a] *ARC Centre of Excellence for Electromaterials Science, Intelligent Polymer Research Institute, AIIM Facility, Innovation Campus, University of Wollongong, NSW 2522, Australia. E-mail: innis@uow.edu.au; Fax: +61 02 4221 3114; Tel: +61 02 4221 4351*
[b] *Biomedical Diagnostics Institute, National Centre for Sensor Research, School of Chemical Sciences, Dublin City University, Dublin 9, Ireland. E-mail: Robert.Forster@dcu.ie; Fax: +353 1 700 5943; Tel: +353 1 7005503*

† Electronic supplementary information (ESI) available: Sterm–Volmer plots and luminescent l. See DOI: 10.1039/c0cp00699h

A-PAni has similar properties to low molecular weight poly(2-methoxyaniline-5-sulfonic acid) (LMWT PMAS) oligomer recently reported by us.[14,15] The polymerisation of methoxyaniline-5-sulfonic acid) (MAS) at a weakly acidic pH of 3.5 has been shown to result in the formation of two fractions that have very different molecular weights and physical properties that require significant effort to separate.[14] LMWT PMAS (molecular weight 2.5 kDa) is non-conductive and redox inert. In contrast, high molecular weight (HMWT) PMAS has a molecular weight of 8–10 kDa and is both conductive and redox active, like most PAni emeraldine salts.[15–17] It has been demonstrated that there is a strong association of both of these PMAS fractions to each other in the as-synthesised polymer in solution and the solid-state which significantly impact upon their electronic character.[15,18] Studies into the interactions of these PMAS fractions have shown that the LMWT oligomer significantly modulates the photochemical and electronic properties of the emeraldine salt.[15,18] PMAS has been shown to effectively quench fluorescent emission of the LMWT PMAS *via* a static (Perrin) energy transfer process.[15]

The magnitude of conductivity in a conducting polymer will be dependent upon the extent of the charge carrier (polaron) delocalisation, the polaron mobility and the presence of structural disorder such as non head-to-tail coupling defects.[19,20] The nature and evolution of high spin radical cations (or polarons) and their shift towards the zero spin dicationic bipolarons in conducting polymers can be examined using electron spin resonance (ESR) and Raman spectroscopy.[21–23] The advantage of ESR is that it directly measures the relative concentration of polaron spin within the polymeric material.[24,25] Raman spectroscopy can also indicate the presence of radical cations and dications (or dianions) in conductive polymers by observing the changes associated with the $C–N^+$ functionality.[26–29]

The influence of the controlled addition of different weight fractions of A-PAni on the unique spectroscopic and electronic properties of PAni will be elucidated within this investigation.

Experimental section

Materials and reagents

Aniline, APS, HCl and NH_4OH and HCSA were purchased from Aldrich. All other reagents used were of analytical grade and solutions were prepared in Milli-Q water (18 MΩ cm). PAni emeraldine salt, (PAni·HCSA) was prepared by chemical polymerisation of a 50 mL aqueous solution containing 0.2 M aniline and 2.0 M camphor sulfonic acid (HCSA) with 50 mL 0.2 M ammonium peroxydisulfate (APS) over 24 hours at room temperature with gentle stirring. The resultant product was filtered and washed with water until a neutral filtrate pH was obtained and then air dried. Alkaline PAni, (A-PAni), was prepared according to a literature method at an initial pH of 3 with typical yields of 70–80%.[8] An aqueous polymerization bath of 0.01 M aniline in the presence of 0.01 M APS and 0.01 M HCl was prepared by adding 10 mL of 0.02 M aniline aqueous solution in 0.01 M HCl to a 30 mL beaker under mild magnetic stirring, followed by the addition of 10 mL of the 0.02 M APS aqueous solution in 0.01 M HCl. To this 1.0 M ammonium hydroxide aqueous solution was added in order to quench the reaction after approximately 12 hours resulting in a yellowish brown coloured aqueous dispersion of product. The resultant product was filtered and washed with water until a neutral filtrate pH was obtained and air dried.

Sample preparation

For ESR studies, mixtures of PAni·HCSA and A-PAni were dissolved in NMP at loading levels shown in Table 1. 20 μL aliquots of these solutions were micropipetted onto the tip of a microcapillary tube, dried and inserted into a 2.0 mm inner diameter ESR tube (Bruker). The ESR tube was then inserted into the ESR spectrometer resonator and left at a fixed position for all subsequent measurements. The microcapillary tubes, rather than the ESR tube were removed from the resonator in order to produce reproducible tuning. Immediately after each ESR study, a Raman spectrum of the deposit at the tip of the microcapillary tube was acquired. All spectra were performed in triplicate.

Samples for electrochemical and spectroscopic investigations were made on ITO conductive glass (Hartford Glass Co. Inc. (Hartford City, Indiana, USA)) that was cut into 0.8 × 2 cm working electrodes. These electrodes were utilized for all UV-vis and Raman analysis. Composite solutions of 1.5 mg mL^{-1} containing PAni·HCSA and A-PAni and 50/50 mixtures, (those used for 50 and 100% samples given in Table 1), of the two in NMP were prepared. Where appropriate, working electrodes were modified by applying a drop (200 μL) of the composite solution to the electrode surface and dried in the dark for 10 to 12 hours. These modified electrodes were then washed (Milli-Q water) and allowed to dry overnight prior to analysis. Post synthesis characterization was performed at room temperature in aqueous 0.1 M H_2SO_4 unless otherwise stated. Surface coverage of the composite films, Γ, were determined by graphical integration of background corrected cyclic voltammograms (<5 mV s^{-1}). The surface coverage for all composite films was $7 \pm 2 \times 10^{-9}$ mol cm^{-2} unless otherwise stated. An ITO modified electrode was used as the working electrode with platinum counter and Ag/AgCl electrode acting as reference electrodes. Electrical conductivity samples were prepared by drop casting (600 μL, ~10 μm thickness)

Table 1 Mixed solutions of PAni·HCSA and A-PAni utilized within this study. Weight ratios are also provided

% PAni·HCSA	Volume A-PAni[a]/μL	Volume PAni·HCSA[b]/μL	Volume NMP/μL	Total volume/μL
100	0	400	0	400
50	200	200	0	400
46.67	200	175	25	400
42.86	200	150	50	400
38.46	200	125	75	400
33.34	200	100	100	400
27.27	200	75	125	400
20	200	50	150	400
11.11	200	25	175	400
0	400	0	0	400

[a] Stock aqueous solution of A-PAni was 1.5 mg mL^{-1}. [b] Stock aqueous solution of PAni·HCSA was 1.5 mg mL^{-1}.

equivalent composite solutions onto a glass substrate, and allowed to dry. Conductivity measurements were then taken at three different points on the film.

Apparatus

ESR spectra were recorded on a Bruker EMX ESR spectrometer under identical conditions: microwave frequency of 9.861 GHz, attenuator of 30.0 dB, sweep width of 30 G, modulation frequency of 100 kHz, modulation amplitude of 1 G, time constant of 40.96 ms, conversion time of 163.84 ms and sweep time of 671 s were employed unless otherwise stated. All spectra were recorded at room temperature.

Raman spectra were recorded on a Jobin Yvon Horiba HR800 Raman microscope. A He-Ne (632.8 nm) laser was utilised with a 300-line grating providing a resolution of ± 1.25 cm^{-1}. Absorbance and photo-luminescence were recorded using a Shimadzu UV-240 spectrophotometer and a Perkin Elmer LS-50 luminescence spectrometer with 370 nm excitation wavelength, respectively. An ITO modified electrode was used as the working electrode, and a platinum flag acted as the counter electrode. Potentials are quoted versus Ag/AgCl and all measurements were made at room temperature, 23 ± 2 °C.

Fluorescence lifetime studies were made on a PicoQuant PDL-800B pulsed diode laser controller and FluoTime 100 time-correlated single photon counting system (TCSPC) with 370 nm pulsed laser source with cut-on filters of 400, 475 and 530 nm. TCSPC analysis was performed using PicoQuant FluoFit software. ITO conductive glass was cut into 0.8×2.0 cm working electrodes. These electrodes were utilized for all spectrochemical analysis. Prior to use working electrodes were rinsed with ethanol, subsequently cleaned with household detergent in water, rinsed with deionised water, followed by acetone and deionised water. Finally, they were gradually heated to 400 °C for 15 min. The electrodes were then dried completely under a flow of nitrogen gas and modified with the PAni composite prior to use. A nitrogen atmosphere was maintained during data collection.

Conductivity measurements were performed on dried films of 10 μm thickness (obtained by evaporative air casting on a glass slide substrate) using a JANDEL resistivity system (model RM2) with a linear four-point probe head.

Results and discussion

ESR analysis

ESR is a very powerful method for studies into the conduction mechanisms of conducting polymers. ESR has been frequently used to investigate the nature of various quasi-particles[30–33] (such as excitons,[31] solitons, polarons,[30] and bipolarons)[32] that can play a range of roles in the electronic charge transport processes in ground and excited states. ESR has also been employed to examine the population and reversible evolution of the polaron to the bipolaron in conducting polymers.[32] Conducting polymers typically display a single broad resonance line located close to the g value of 2.003 which has been assigned to the presence of the non-spin paired ($s = \frac{1}{2}$) polaron.[24,33–35] At higher levels of oxidation, polarons have been observed to spin pair, forming the zero spin ($s = 0$) bipolaron state which presents no ESR spectrum.[36,37] The observed magnetic properties of the emeraldine salt form of PAni are therefore due to polaron spins (radical cations). However, if different oligomers and isomers such as the A-PAni are present different ESR spectra may arise due to different chemical environments.

In this work PAni·HCSA exhibits an ESR singlet, with a g factor of *ca.* ~2.0045 g, and a line width (ΔH) of 3.483 G, as shown in Fig. 1. This was close to the free electron g value (2.0023) indicative of resonance that comes from electrons delocalised in the π-system of the carbon atoms forming the polymer backbone in the main chain.[38–43] The ESR spectra showed no hyperfine structure, which is characteristic of delocalised free radicals that exist along the polymer backbone.[44] As with previously published work, the intensity was comparable to those observed for primary doped PAni, with the peak to peak line-widths also indicating a high electronic delocalisation which is consistent with a more extended conformation of the polymeric chains.[26,45]

No ESR response was observed for A-PAni, however this does not necessarily indicate the presence of spinless bipolarons in this material. A-PAni was shown to be redox inactive (see Fig. 3 and later discussion), suggesting that the reported phenazine-like defects[7,46,47] in the A-PAni oligomer were incapable of supporting a delocalised polaron due to the break in conjugation resulting from these defects.

Unexpectedly, the intensity of the ESR signal was found to increase linearly with decreasing amounts of PAni·HCSA at fixed A-PAni loadings, as shown in Fig. 1. Spin concentration, indicative of the relative population of the number of non-spin paired electrons, can be estimated by the double integration of the observed ESR signal. A decrease in spin concentration would have been predicted as the amount of high spin

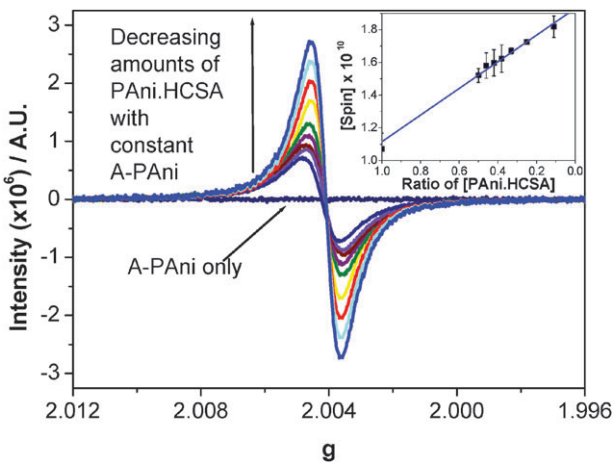

Fig. 1 Influence of the presence of A-PAni, on the ESR spectra of solid state samples of decreasing PAni–HCSA content with constant loading of A-PAni, based on total polymer content. Microwave frequency of 9.861 GHz, attenuator of 30.0 dB, sweep width of 70 G, modulation frequency of 100 kHz, modulation amplitude of 0.25 G, time constant of 5.12 ms, conversion time of 20.48 ms and sweep time of 20.97 s were employed. Insert plots the influence of increasing amounts of A-PAni on spin concentration of the PAni–HCSA samples shown in this Figure.

PAni·HCSA in the mixture decreased thereby reducing the number of polarons present in the solid state sample. However, the observed increase in spin intensity (Fig. 1 and inset), did not correlate to a simple dilution effect. The spin concentration of emeraldine salt of the PAni·HCSA was found to be $\sim(1.2 \pm 0.6) \times 10^{10}$ for 0.06 mg in the ESR cavity.

In a comparative study PAni·HCSA was diluted with a fully sulfonated 2 kDa polystyrenesulfonate (PSS) oligomer (Fig. 2). PSS was chosen as a non-conducting but doping analogue to the A-PAni component. The incorporation of PSS with PAni·HCSA in the solid state showed the predicted decrease in spin concentration as the amount of high spin PAni·HCSA was reduced, Fig. 3 and inset. However, this decrease in spin concentration was in sharp contrast to the increase that was observed upon addition of A-PAni. Interestingly, solution state studies of these mixtures with PSS or A-PAni did not influence the high spin ESR signal observed for the PAni·HCSA fraction, again other than the expected dilution effects. This result was similar to previous studies reported on the interaction of PMAS fractions.[18]

The increase in spin concentration implies that the A-PAni interacts with the PAni·HCSA in such a way as to create a composite material with a higher overall spin state. This result was inconsistent with previous work performed on the interactions of two fractions of PMAS, which showed a dramatic decrease in spin concentration, significantly without a change in the PMAS oxidation state, to form bipolaronic states.[18] Importantly, the increase in electron spin provides strong evidence that A-PAni does not behave like an inert filler, as was the case for PSS. A-PAni itself was shown to be redox and ESR inactive, Fig. 3, and therefore is unlikely to act as an internal oxidant leading to the formation of additional radical cations in the PAni·HCSA. As reported for the PMAS LMWT analogues,[18] a change in spin concentration does not necessarily indicate a change in the oxidation state of the polymer. A more

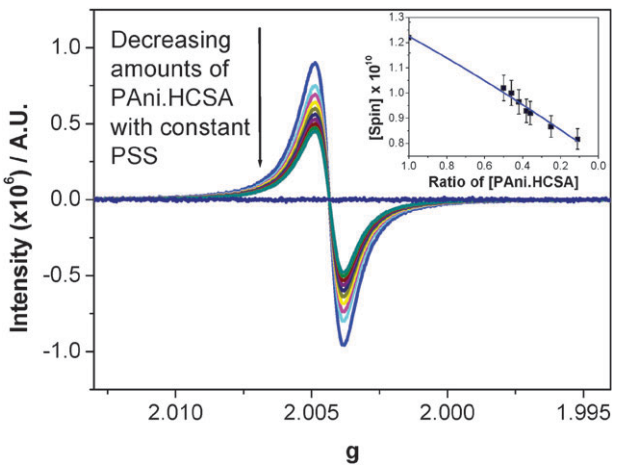

Fig. 2 Typical ESR responses of solid state samples of decreasing PAni–HCSA emeraldine salt content with constant loading of PSS. The overall polymer concentration was kept constant with the ratio of the two fractions changing. A microwave frequency of 9.861 GHz, attenuator of 30.0 dB, sweep width of 70 G, modulation frequency of 100 kHz, modulation amplitude of 0.25 G, time constant of 40.96 ms, conversion time of 163.84 ms and sweep time of 671 s were employed.

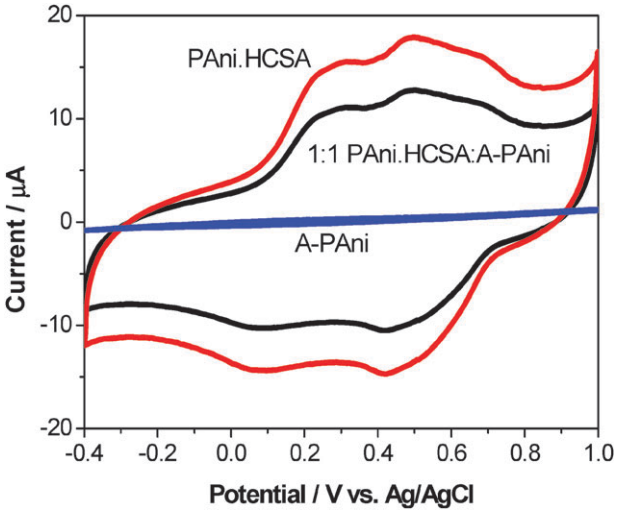

Fig. 3 Typical cyclic voltammograms of thin films of: (black) PAni·HCSA emeraldine salt, (blue), A-PAni and (red) a 1 : 1 mixture of PAni·HCSA and A-PAni, on ITO electrodes. Electrolyte was 0.1 M H_2SO_4, and a scan rate of 100 mV s^{-1} was used. The surface coverage for both was $6 \pm 2 \times 10^{-9}$ mol cm^{-2}. Cyclic voltammograms were recorded over the range $-100 \leq E\,(\text{mV}) \geq 900$ with the CV starting at -100 mV.

probable explanation is that the interaction of polarons and bipolarons is an equilibrium process. The results presented here would suggest that A-PAni shifts this equilibrium in favour of polaron formation (or bipolaron dissociation) as these materials interact in the solid-state (see later discussions).

Electrochemical properties of the conducting polymer films

The conducting polymer films exhibit quasi-reversible chemistry as illustrated in Fig. 3. Cyclic voltammograms obtained for PAni·HCSA with the main peaks corresponding to the transformation of leucoemeraldine base to emeraldine salt and the emeraldine salt to pernigraniline salt, respectively. On the reverse scan, the oxidation peaks correspond to the conversion of pernigraniline salt to emeraldine salt and emeraldine salt to leucoemeraldine base. The electrochemical properties display features typical of surface confined redox sites similar to those previously reported.[16,48–50] The film consisting of A-PAni showed no redox activity, similar to low molecular weight PMAS. Films containing a mixture of the two polymers, showed the typical response of the PAni emeraldine salt although with a corresponding current reduction due to having half the amount of PAni·HCSA in the film.

Conductivity

The electrical conductivity of a conducting polymer is intrinsically related to the concentration and mobility of the polaron and bipolaron charge carriers on the polymer backbone. Conduction is not only dependant on the ability for charge to pass along individual polymer chains (*intra* charge transfer) but also to pass between adjacent chains (*inter* charge transfer). For charge conduction in composites containing conducting polymers the weight fraction of the conducting component must be high enough to ensure

the presence of an electrical pathway between each of the conducting domains within the insulating matrix. The critical concentration of the conducting component, above which significant improvements in charge transfer are enabled, is called the percolation threshold. For PAni composites, the percolation threshold can vary depending on the dopant utilised, however most range from 10 to 25 w/w % of the PAni electroactive component. As such, the final conductivity of the composite will depend on both the base conductivity of the conductor as well as the ability for charge to transfer between each of the conducting domains.

The conductivities of as-cast composite films containing different weight fractions of PAni to the insulating filler of both PSS and A-PAni may be seen in Fig. 4. Electrical conductivities of 2.22 S cm^{-1} were observed for films containing 100% of the PAni·HCSA fraction. The PSS based films displayed a slow decrease in conductivity until a significant drop was seen for PAni weight fractions below 20%. This was attributed to a drop below percolation. In contrast, the A-PAni film conductivities remained relatively consistent for each of the weight fractions investigated. No sharp percolation threshold was observed and only a slight decrease in conductivity was seen where films containing 11% PAni·HCSA still had conductivities of 1.22 S cm^{-1}

The absence of a percolation threshold for the sample with the A-PAni films present suggests that the A-PAni matrix within the composite was not acting as a purely insulating matrix but dramatically influences the electronic character of the PAni·HCSA component within the film. This finding was consistent with the unexpected shift to produce more polarons rather than bipolarons demonstrated in the ESR study. Such a phenomenon may improve the intra charge transfer along individual polymer chains within the PAni·HCSA components of the film. In order to achieve this effect the A-PAni upon interaction with the PAni·HCSA appears to induce a pseudo-doping effect within the composite.

Raman spectroscopy

Raman spectroscopy is a very efficient tool for characterising radical cations and dications or dianions in intrinsically conductive polymers, including PAni.[51] Information about the amount and nature of particular groups allows the determination of the structural disorder of the conducting polymer. Depending on the degree of conjugation of each group, their vibrational frequencies will be different, leading to a broadening of the Raman band indicating a considerable degree of disorder in the polymer material.[52] Fig. 5 shows the Raman spectra solid-state samples of the emeraldine salt form of PAni·HCSA, A-PAni and the composite containing both fractions in a 1 : 1 weight ratio. The range 1100 to 1700 cm^{-1} corresponds to the stretching modes of different bonds. The different modes of vibration can be interpreted separately; the C–H bending modes between 1100 and 1210 cm^{-1}, the different C–N stretching modes (amines, imines, polarons) between 1210 and 1520 cm^{-1} , and the ring C=C quinoid stretching mode *ca.* 1590 cm^{-1}.

The Raman spectrum of PAni·HCSA shows a broad polaron doublet, with components at 1386 and 1415 cm^{-1} associated with the presence of C–$N^{\bullet+}$ polaron.[28,29,53,54] This doublet is close to those observed for the Raman spectrum of metallic PAni.[55] The key difference in the A-PAni spectra shows a peak at 1482 cm^{-1} associated with the quinoid ring vibrational modes (C=N) typically found in phenazines[54] and the unprotonated imine typically seen in non-conducting emeraldine base.[28,56,57]

The spectra of PAni·HCSA and 1 : 1 PAni·HCSA:PSS shown in Fig. 6, show similar stretching modes and are consistent with the ESR results that PSS acts as an inert filler. Both show characteristic bands typical of the PAni·HCSA already described. The Raman spectrum recorded for PSS did show bands consistent with C=C stretching, C–H stretching and bending modes and ring deformation modes that were all negligible compared to the responses of both fractions of PAni.

Upon addition of the A-PAni to PAni·HCSA there was a slight increase in the intensity of the band centred at 1597 cm^{-1}, which was indicative of the C=C stretching in the benzoid rings of PAni ES. Accompanying these changes was also an increase in the C=N vibrational modes at 1482 cm^{-1}.[28,54,56,57] However, there was no clear change in

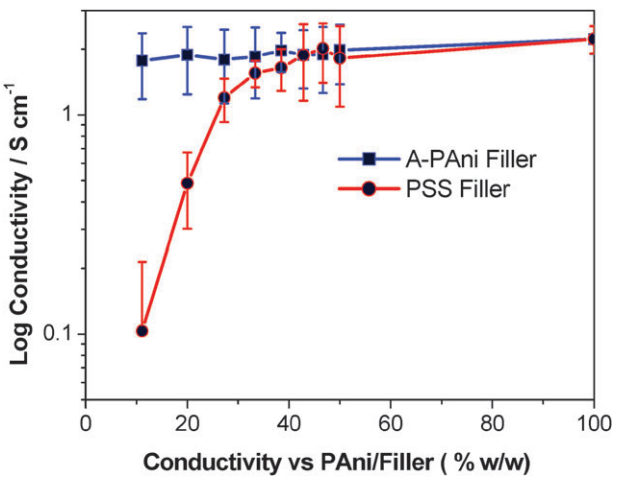

Fig. 4 Conductivity *vs.* %PAni–HCSA for (blue) A-PAni and (pink) PSS content in composite films.

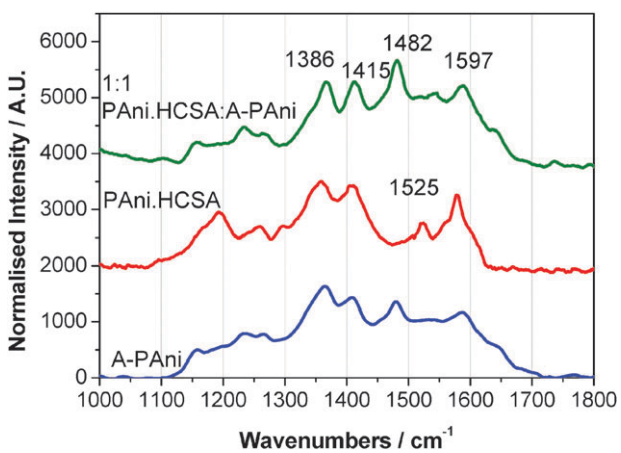

Fig. 5 Raman spectra of: (a) PAni–HCSA emeraldine salt only, (b) A-PAni only and (c) a 1 : 1 mixture of PAni–HCSA and A-PAni. A 632.8 nm laser was utilised as the incident excitation.

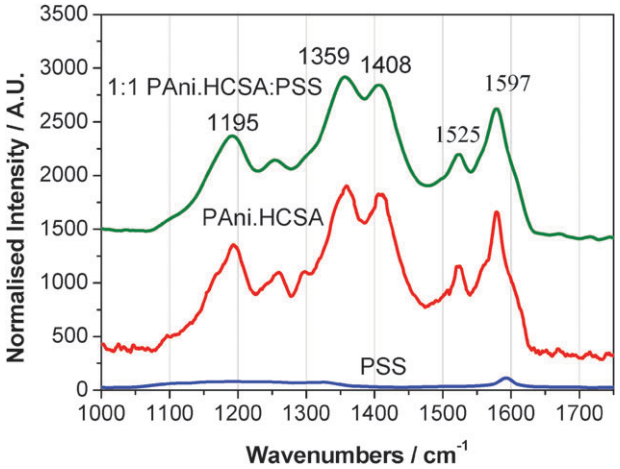

Fig. 6 Raman spectra of: (a) PSS only, (b) PAni–HCSA emeraldine salt only and (c) a 1 : 1 mixture of PAni–HCSA and PSS. A 632.8 nm laser was utilised as the incident excitation.

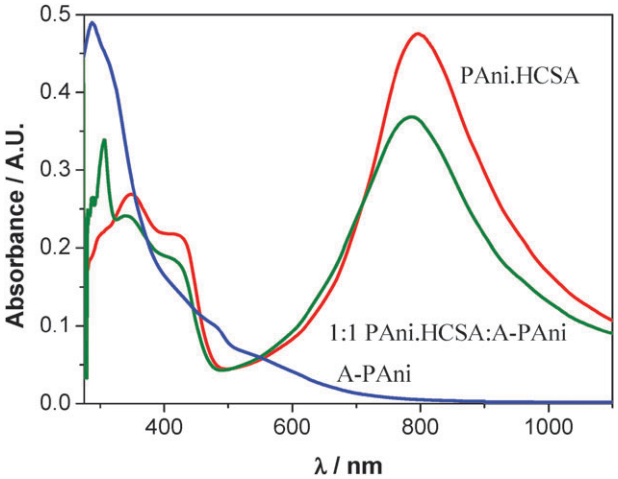

Fig. 7 UV-visible spectra of three films, containing (a) PAni–HCSA emeraldine salt only, (b) A-PAni only and (c) a 1 : 1 mixture of PAni–HCSA and A-PAni. The surface coverage for all composite films was $6.7 \pm 2 \times 10^{-9}$ mol cm^{-2}.

the intensity of the polaron bands at 1386 and 1415 cm^{-1}. Significantly, these polaron bands intensities were maintained in the 50 : 50 composite. In contrast to these findings, previous studies probing the influence of LMWT PMAS on the emeraldine salt form of PMAS, has demonstrated the loss of these features due to a shift to the bipolaronic charge carrier state.[18]

Absorption analysis

Fig. 7 shows the typical UV-Vis spectrum of PAni·HCSA, with three distinctive absorption bands at approximately 350 nm, a shoulder at 430 nm and 800 nm corresponding to π–π* transitions, polaronic and bipolaronic bands.[58] The λ_{max} values are slightly shifted compared to solution phase spectra which is consistent with previous studies.[59] These are in agreement with a localised polaron structure and a coil like conformation of the polymer chain. The UV-Vis absorption of A-PAni is also illustrated with the most prominent absorption band at approximately 290 nm, typical of a π–π* transition. The spectra of the mixed film is also shown in Fig. 7, the polaron absorption band is higher than would be expected. However, this is in agreement with the ESR and Raman data that indicate the addition of A-PAni to PAni·HCSA reults in an increase in high spin polarons within the composite material.

These results illustrate the extent to which the two fractions interact with one another, impacting greatly on their physical properties. Both the Raman and ESR spectra show the dramatic increase in spin/polaron concentration of PAni·HCSA upon interaction with A-PAni.

Steady state luminescence of composites of PAni·HCSA and A-PAni

As with the conductivity, these interactions significantly affect the luminescence properties of PAni. Fig. 8 shows that the emission intensity of A-PAni decreases upon addition of the PAni·HCSA quencher in the solid state. This quenching response can be described by the Stern–Volmer equation:

$$I_o/I = 1 + K_{SV}[Q] \quad (1)$$

where I_o and I are the fluorescence intensities in the absence and presence of quencher respectively and K_{SV} is the Stern–Volmer constant. In systems of this kind, quenching has been attributed to the interaction of singlet excitons in the photoexcited state with polarons.[60,61] A-PAni exhibited a photoluminescence band with a peak maximum centered at ~520 nm, and a weak shoulder observed at ~460 nm. In contrast, PAni·HCSA shows a substantially weaker photoluminescence, as expected for an emeraldine salt.

In analysing the emission intensity data, it is important to correct for absorbances at the excitation wavelength as the quencher is added. This was accomplished using standard procedures, according to eqn (2)[62,63] where $(I_0/I)_{app}$ is the ratio of the emission intensity with and without the quencher, and A_D and A_Q are the absorbance of the donor and quencher, respectively at the excitation wavelength. Fig. S1 (ESI†) shows that after correcting for this effect, the Stern–Volmer plot

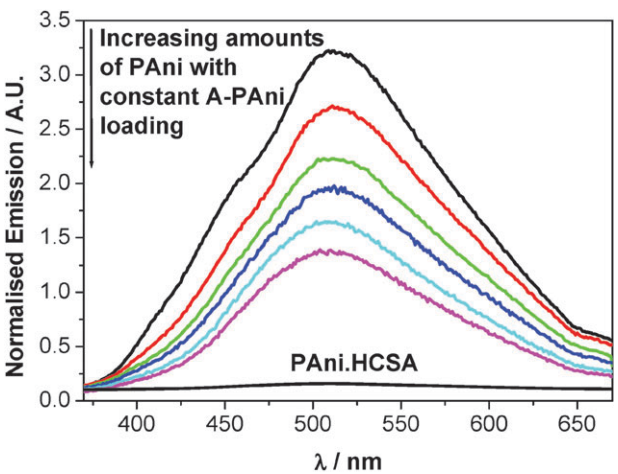

Fig. 8 Typical solid state luminescence spectra for composite films, containing constant [A-PAni] with increasing amounts of PAni·HCSA. Excitation wavelength of 370 nm was utilised.

is linear response and that the Stern–Volmer constant is $57 \pm 6\ M^{-1}$.

$$\left(\frac{I_0}{I}\right)_{corr} = \left(\frac{I_0}{I}\right)_{app}\left[\frac{1-10^{-(A_D+A_Q)}}{1-10^{-A_D}}\right]\frac{A_D}{(A_D+A_Q)} \qquad (2)$$

The quenching efficiency can be calculated from the decrease of the donor emission using eqn (3), where I_{DA} is the intensity of the donor–acceptor pair and I_D is that of the donor alone. The quenching efficiency was found to be approximately 56% at a mole ratio of 2.

$$E_Q = \left(\frac{1-I_{DA}}{I_{DA}}\right) \qquad (3)$$

These results would suggest that a dynamic quenching effect occurs when the PAni·HCSA was added to A-PAni, a result that was in direct contrast to the static (Perrin) mechanism observed for PMAS mixtures.[18] Dynamic quenching behaviour is typified by a collision encounter of the quencher (PAni·HCSA) with the luminescent complex (A-PAni); however such behaviour would be unexpected in solid-state samples. In this instance it is not a discrete bimolecular molecular motion, characteristic of solution based quenching, that drives this process. Rather, it is the ability of the mobile polaron and bipolaron quenchers[60,61] to move along the conjugated PAni ES backbone, in the solid state, and interact with the A-PAni luminophore to quench its response.

Comparison of these results to solution phase data was not possible due to the solubility limitations required to dissolve sufficiently high concentrations of both polymers to achieve significant quenching.

Luminescence lifetimes of composites

The luminescent lifetime can provide useful insights into the mechanism of excited state energy transfer between the fluorophore and the quencher. A time-correlated single photon counting (TCSPC) system was employed using 370 nm pulsed laser sources with a cut-on filter of 400 nm. Typical TCSPC responses for A-PAni quenched by the addition of PAni·HCSA, (Fig. S2, ESI†). In each instance, the trace relates to the TCSPC output and the resultant model fit. The TCSPC responses in each case were collected to the same photon count intensity, (10 000 counts). Emission responses were analyzed using PicoQuant FluoFit software employing a fitting function containing two time constants.

A-PAni exhibits an exponential decay in the solid state with a lifetime of ~8 ns. A typical Stern–Volmer plot for luminescence lifetime, τ_0/τ *versus* [*Q*], where τ_0 and τ are the lifetimes in the absence and presence of the quencher, is shown in the inset in Fig. S2 (ESI†). When luminescence quenching occurs *via* a pure dynamic quenching process the slopes of plots of I_0/I and τ_0/τ should be identical and the Stern–Volmer constant, K_{SV}, is equal to k_q. Fig. S1 (ESI†) shows that the slopes of the intensity and lifetime Stern–Volmer plots are 57.2 ± 6 and 31.3 ± 4.1, respectively. The fact that these slopes differ from one another indicates that while dynamic quenching occurs in this system to an extent, it does not fully account for the decrease in emission observed. Therefore, it appears that while collisional quenching occurs, static quenching is also a contributing factor. This conclusion appears reasonable given that the luminophores and quenchers are both confined to the electrode surface and physical displacement will involve at least segmental polymer chain movement of the PAni composite.

Conclusions

The influence of a non-conducting, redox inactive oligomer (A-PAni) on the electronic properties of PAni·HCSA is examined. Results indicate that there is a strong electronic interaction between the two forms of PAni which impacts considerably on their individual properties. The addition of A-PAni results in a smaller than expected decrease in electrical conductivity for the incorporation of an insulating, inert filler. Accompanying this was an increase in electron spin associated with the presence of the polaronic charge carrier, as confirmed by ESR and Raman spectroscopy.

These findings indicate that the non-conducting A-PAni fraction interacts strongly, in the solid-state, with the electronic structure of the PAni·HCSA to enhance the intra-chain and inter-chain charge transfer processes within the PAni·HCSA. This may be through a pseudo-doping of the A-PAni. Importantly, the interactions of these two materials in the solid-state are not purely static in nature but rather a mixed static-dynamic process.

This contribution illustrates the unusual chemistry of these two related materials when they interact with one another. The pH dependant nature of PAni during synthesis in all its forms leads to the conclusion that the formation of A-PAni may be an inherent by-product of polyaniline synthesis. The A-PAni has been shown to ultimately affect the nature and quality of the final polymer product. The lack of homogeneity in polyaniline synthesis, even within the same laboratory utilising the same methodology, may be reason enough to consider furthering research into A-PAni.

Acknowledgements

The continued financial assistance from the Australian Research Council under the ARC Centres of Excellence programs, QE(II) Fellowship (Innis) and the ARC Australian Research Network for Advanced Materials (ARNAM Travel Fellowship, Dennany) programmes is also greatly appreciated. The financial support of Science Foundation Ireland under the Biomedical Diagnostics Institute (Award No. 05/CE3/B754) is deeply appreciated.

References

1 D. M. Mohilner, R. N. Adams and W. J. Argersinger, *J. Am. Chem. Soc.*, 1962, **84**, 3618–3622.
2 D. E. Stilwell and S.-M. Park, *J. Electrochem. Soc.*, 1988, **135**, 2491–2502.
3 A. Kitani, K. Masanoir and K. Sasaki, *J. Electrochem. Soc.*, 1986, **133**, 1069–1073.
4 S. Gottesfeld, A. Redondo and S. W. Feldberg, *J. Electrochem. Soc.*, 1987, **134**, 271–272.
5 A. G. MacDiarmid, *Angew. Chem., Int. Ed.*, 2001, **40**, 2581.
6 C. O. Baker, B. Shedd, P. C. Innis, P. G. Whitten, G. M. Spinks, G. G. Wallace and R. B. Kaner, *Adv. Mater.*, 2008, **20**, 155–158.
7 I. Sapurina and J. Stejskal, *Polym. Int.*, 2008, **57**, 1295–1325.

8 E. C. Venancio, P.-C. Wang and A. G. MacDiarmid, *Synth. Met.*, 2006, **156**, 357–369.
9 E. C. Venancio, P.-C. Wang, O. Y. Toledo and A. G. MacDiarmid, *Synth. Met.*, 2007, **157**, 758–763.
10 W. H. Pirkle and J. C. Stickler, *J. Am. Chem. Soc.*, 1970, **92**, 7497–7499.
11 P. A. S. Smith, *Derivatives of Hydrazine and Other Hydronitrogens Having N–N bonds*, The Benjamin/Cummings Publishing Co., Reading, 1983.
12 X. Wang, N. Liu, W. Zhang and Y. Wei, *Chem. Lett.*, 2005, **34**, 42–43.
13 J. Huang and R. B. Kaner, *J. Am. Chem. Soc.*, 2004, **126**, 851–855.
14 F. Masdarolomoor, P. C. Innis, S. Ashraf and G. G. Wallace, *Synth. Met.*, 2005, **153**, 181–184.
15 P. C. Innis, F. Masdarolomoor, L. A. P. Kane-Maguire, R. J. Forster, T. E. Keyes and G. G. Wallace, *J. Phys. Chem. B*, 2007, **111**, 12738–12747.
16 F. Masdarolomoor, P. C. Innis, S. Ashraf and G. G. Wallace, *Synth. Met.*, 2005, **153**, 181–184.
17 L. A. P. Kane-Maguire, J. A. Causley, N. A. P. Kane-Maguire and G. G. Wallace, *Curr. Appl. Phys.*, 2004, **4**, 394–397.
18 L. Dennany, P. C. Innis, F. Masdarolomoor and G. G. Wallace, *J. Phys. Chem. B*, 2010, **114**, 2337–2341.
19 A. J. Epstein, J. M. Ginder, F. Zuo, R. W. Bigelow, H. S. Woo, D. B. Tanner, A. F. Richter, W.-S. Huang and A. G. MacDiarmid, *Synth. Met.*, 1987, **18**, 303–309.
20 J. M. Ginder, A. F. Richter, A. G. MacDiarmid and A. J. Epstein, *Solid State Commun.*, 1987, **63**, 97–98.
21 Y. Furukawa, *Synth. Met.*, 1995, **69**, 629–632.
22 Y. Furukawa, A. Sakamoto, H. Ohta and M. Tasumi, *Synth. Met.*, 1992, **49**, 335–340.
23 S. Mu, J. Kan, J. Lu and L. Zhuang, *J. Electroanal. Chem.*, 1998, **446**, 107–112.
24 P. K. Kahol, *Solid State Commun.*, 2000, **117**, 37–39.
25 P. K. Kahol, A. J. Dyakonov and B. J. McCormick, *Synth. Met.*, 1997, **89**, 17–28.
26 J. E. Pereira da Silva, M. L. A. Temperini and S. I. Cordoba de Torresi, *Electrochim. Acta*, 1999, **44**, 1887–1891.
27 T. Fukuda, H. Takezoe, K. Ishikawa, A. Fukuda, H. S. Woo, S. K. Jeong, E. J. Oh and J. S. Suh, *Synth. Met.*, 1995, **69**, 175–176.
28 M. C. Bernard and A. Hugot-Le Goff, *Electrochim. Acta*, 2006, **52**, 595–603.
29 M. C. Bernard and A. Hugot-Le Goff, *Electrochim. Acta*, 2006, **52**, 728–735.
30 P. L. Pratt, S. J. Blundell, H. W. K. Nagamine, K. Ishida and A. P. Monkman, *Phys. Rev. Lett.*, 1997, **79**, 2855–2859.
31 J. S. Salafsky, *Phys. Rev. B: Condens. Matter*, 1999, **59**, 10885–10894.
32 S. Charkrabarti, B. Das, P. Banerji, D. Banerjee and R. Bhattacharya, *Phys. Rev. B: Condens. Matter*, 1999, **60**, 7691–7694.
33 M. Chipara, D. Hui, P. V. Notingher, M. D. Chipara, K. T. Lau, J. Sankar and D. Panaitescu, *Composites, Part B*, 2003, **34**, 637–645.
34 J. Lippe and R. Holze, *Synth. Met.*, 1991, **43**, 2927–2930.
35 S. M. Yang and C. P. Li, *Synth. Met.*, 1993, **55**, 636–641.
36 V. Luthra, R. Singh, S. K. Gupta and A. Mansingh, *Curr. Appl. Phys.*, 2003, **3**, 219–222.
37 F. Lux, *Polymer*, 1994, **35**, 2915–2936.
38 F. Lafolet, F. Genoud, B. Divisia-Blohorn, C. Aronica and S. Guillerez, *J. Phys. Chem. B*, 2005, **109**, 12755–12761.
39 G. Zotti, G. Schiavon, S. Zecchin, A. Berlin, G. Pagani and A. Canavesi, *Synth. Met.*, 1996, **76**, 255–258.
40 Q. Zhou, L. Zhuang and J. Lu, *Electrochem. Commun.*, 2002, **4**, 733–736.
41 I. Y. Sakharov, I. V. Ouporov, A. K. Vorobiev, M. G. Roig and O. Y. Pletjushkina, *Synth. Met.*, 2004, **142**, 127–135.
42 S.-A. Chen and G.-W. Hwang, *Macromolecules*, 1996, **29**, 3950–3955.
43 L. Dennany, P. Sherrell, J. Chen, P. C. Innis, G. G. Wallace and A. I. Minett, *Phys. Chem. Chem. Phys.*, 2010, **12**, 4135–4141.
44 K. Takahashi, K. Nakamura, T. Yamaguchi, T. Komura, S. Ito, R. Aizawa and K. Murata, *Synth. Met.*, 2002, **128**, 27–33.
45 J. E. Pereira da Silva, D. L. A. de Faria, S. I. Cordoba de Torresi and M. L. A. Temperini, *Macromolecules*, 2000, **33**, 3077–3083.
46 J. Stejskal, I. Sapurina, M. Trchova, E. N. Konyushenko and P. Holler, *Polymer*, 2006, **47**, 8253–8262.
47 J. Stejskal, I. Sapurina, M. Trchova and E. N. Konyushenko, *Macromolecules*, 2008, **41**, 3530–3536.
48 L. Dennany, E. J. O'Reilly, P. C. Innis, G. G. Wallace and R. J. Forster, *Electrochim. Acta*, 2007, **53**, 4599–4605.
49 L. Dennany, R. J. Forster and J. F. Rusling, *J. Am. Chem. Soc.*, 2003, **125**, 5213–5218.
50 L. Dennany, G. G. Wallace and R. J. Forster, *Langmuir*, 2009, **25**, 14053–14060.
51 H. G. M. Edwards, A. F. Johnston and I. R. Lewis, *J. Raman Spectrosc.*, 1993, **24**, 475.
52 J. E. Pereira da Silva, M. L. A. Temperini and S. I. Cordoba de Torresi, *Electrochim. Acta*, 1999, **44**, 1887–1891.
53 M. C. Bernard, A. Hugot-Le Goff, H. Arkoub and B. Saïdani, *Electrochim. Acta*, 2007, **52**, 5030–5038.
54 G. Ciric-Marjanovic, M. Trchova and J. Stejskal, *J. Raman Spectrosc.*, 2008, **39**, 1375–1378.
55 C. Engert, S. Umapathy, W. Kiefer and H. Hamaguchi, *Chem. Phys. Lett.*, 1994, **218**, 87–92.
56 G. Niaura, R. Mazeikiene and A. Malinauskas, *Synth. Met.*, 2004, **145**, 105–112.
57 S. Quillard, G. Louarn, S. Lefrant and A. G. Macdiarmid, *Phys. Rev. B: Condens. Matter*, 1994, **50**, 12496.
58 Y. Xia, J. M. Wiesinger, A. G. MacDiarmid and A. J. Epstein, *Chem. Mater.*, 1995, **7**, 443–445.
59 L. Dennany, C. F. Hogan, T. E. Keyes and R. J. Forster, *Anal. Chem.*, 2006, **78**, 1412–1417.
60 Y. Son, H. H. Patterson and C. M. Carlin, *Chem. Phys. Lett.*, 1989, **162**, 461–466.
61 S. Lee, J. Y. Lee and H. Lee, *Synth. Met.*, 1999, **101**, 248–249.
62 J. N. Demas and A. W. Adamson, *J. Am. Chem. Soc.*, 1973, **95**, 5159–5168.
63 G. Navon and N. Sutin, *Inorg. Chem.*, 1974, **13**, 2159–2164.

